Supplemental Materials

Table S1 Interactions of CD82 C-terminal cytoplasmic domain with AP complex μ subunits in yeast two-hybrid system*

	μ1A	μ1B	μ2	μ3A	μ3B	μ4	VP16 vector
TGN38	N.D.	N.D.	+	N.D.	N.D.	N.D.	-
CD63	-	-	-	+	+	-	-
CD82	-	-	-	-	-	-	-

*The interactions were examined in three individual experiments, and the results were consistent among all experiments. The positive interaction denotes the growth in histidine /tryptophan /leucine drop-out plate and the presence of galactosidase activity, reflected by blue colonies, in X-α-Gal indicator histidine /tryptophan /leucine drop-out plate.

To test whether CD82 endocytosis is mediated by clathrin-coated pits through interaction with μ subunits of AP complexes, we used the yeast two-hybrid system to determine whether the CD82 C-terminal cytoplasmic domain that contains the YXXΦ motif can interact with μ subunits.

Interactions between the μ subunits of AP complexes and wild type or mutated C-terminal cytoplasmic domain of CD82 were investigated in yeast two-hybrid system as described elsewhere (Rous et al., 2002; Zhang and Hemler, 1999). The constructs encoding μ1A, μ2, μ3A, μ3B, and μ4 subunits in vector pVP16 that contained a two-hybrid transcriptional activation domain were kindly provided by Dr. J. Paul Luzio (University of Cambridge, Cambridge, UK). The μ1B coding sequence in pACT2 vector was subcloned into pVP16 vector via PCR and ligation. The wild-type (RHVHSEDYSKVPKY) and Yava mutant (RHVHSEDASKAPKY) of the C-teiminal cytoplasmic tail of CD82 were amplified by PCR and constructed into vector pBTM116 that contains a two-hybrid DNA-binding domain. Other pBTM116 constructs used in this study included pBTM116-CD63 C-terminal tail (provided by Dr. J. Paul Luzio) and pBTM116-TGN38 cytoplasmic tail. The interactions between CD63 C-terminal tail and μ3A or μ3B subunits and between TGN38 tail and μ2

subunit were used as positive interaction controls, while the interactions with empty vector pVP16 were negative controls. The yeast strain L40 (Invitrogen) was cotransformed with bait and prey plasmids by using a polyethylene glycol-lithium acetate procedure and plated onto the medium lacking leucine and tryptophan to select the colonies containing both plasmids. These colonies were further selected for 4-7 days on the media 1) lacking leucine, tryptophan, and histidine for the growth and 2) containing X-gal but lacking leucine, tryptophan, and histidine for the β-galactosidase activity.

We found that no direct biochemical interactions occurred between the C-terminal cytoplasmic tail of CD82 and any of μ1A, μ1B, μ2, μ3A or μ3B, and μ4 subunits of adaptor protein complexes in the yeast two-hybrid system. The YXXΦ motif-containing cytoplasmic domains of TGN38, a μ2 subunit-interacting protein (Ohno, 1995; Stephens and Banting, 1998), and of CD63, a μ3 subunit-interacting protein (Rous et al., 2002), bind to the μ2 and μ3 subunits in the yeast two-hybrid system, respectively, as expected.

References

Ohno, H. (1995) Interaction of tyrosine-based sorting signals with clathrin-associated proteins. *Science* **269,** 1872–1875.

Rous, B.A., B.J. Reaves, G. Ihrke, J.A.G. Briggs, S.R. Gray, D.J. Stephens, G. Banting, and J.P. Luzio. (2002). Role of Adaptor Complex AP-3 in Targeting Wild-Type and Mutated CD63 to Lysosomes. **13**, 1071-1082.

Stephens, D. J., and Banting, G. (1998) Specificity of interaction between adaptor-complex medium chains and the tyrosine-based sorting motifs of TGN38 and lgp120. *Biochem. J.* **335,** 567–572.

Zhang, X. A., and Hemler, M. E. (1999) Interaction of the integrin β1 cytoplasmic domain with ICAP-1 protein. *J. Biol. Chem.* **274,** 11–19

Table S2 The colocalization of CD82 with GM1 or caveolin-1

CD82 staining	GM1 (%)*	caveolin-1 (%)*
Distribution (pretreated with)		
Control mAb at 4°C	22.3±2.8	10.9±5.7
CD82 mAb at 4°C	19.2±3.0	6.4±4.4
Internalization		
2 min	0	N/A
30 min	19.2±7.0	6.6±2.9

*The colocalization of CD82 with GM1 or caveolin-1 was quantified by measuring the colocalized pixel areas of immunofluorescent confocal images in Adobe Photoshop. The colocalization results are presented as the percentage of colocalized CD82 pixels from total or internalized CD82 pixels for the steady-state distribution or internalization, respectively, and denote the average ± standard error of three individual experiments. Approximately 20 Du145-CD82 cells were analyzed in each measurement. GM1 was probed with CTxB and caveolin-1 with its Ab.

Figure S1 Endocytotic kinetics of CD82 and EGF-stimulated CD82 endocytosis. A. Du145-CD82 cells were detached and incubated with FITC-conjugated CD82 mAb TS82b or its Fab fragment at 4°C for 1 h and then incubated at 37°C for different time periods for internalization. After acidic washes, the cells were fixed with 3% paraformaldehyde and analyzed with flow cytometry. The internalization rates were calculated as described in Materials and Methods. The results represent the mean of three independent experiments ± standard error. **B**. CD82 endocytosis was analyzed in PrEC-NH cells in the presence or absence of EGF (40 ng/ml) at 37°C for 1 h as described in Materials and Methods.

Figure S2 Additional controls for the analysis of dynamin's role in CD82 endocytosis. A. The effect of dynamin K44A mutant on transferrin endocytosis. Du145-CD82 cells transiently transfected with dynamin wild type-GFP or dynamin dominant negative mutant K44A-GFP fusion were incubated with Alexa 594-conjugated transferrin at 4°C for 60 min. After PBS washes to remove unbound transferrin, the cells were incubated at 37°C for 5 min, followed by acidic washes to remove the cell surface-bound transferrin. The cells were fixed, permeabilized, and analyzed by confocal microscopy. Scale bar, 10 μm. **B.** The effect of acid stripping on CD82 staining in U937 cells. The U937 cells expressing dynamin-GFP fusions were incubated with CD82 mAb M104 at 4°C for 60 min, followed by PBS washes to remove unbound CD82 mAb. The cells were fixed either immediately or after acidic washes to remove the cell surface-bound CD82 mAb. After incubated with Alexa 594-conjugated 2nd Ab, the cells were analyzed by confocal microscopy. Scale bar, 10 μm.

Figure S3 The effects of potassium depletion, cellular acidification, and Eps15 mutants on CD82 endocytosis. A. For potassium depletion experiments, Du145-CD82 cells were shocked in hypotonic serum-free DMEM at 37^{o} for 5 min, washed once with K^{+}-

free isotonic buffer (100 mM NaCl, 50 mM Hepes acid at pH7.4), and then incubated with flurochrome-conjugated CD82 mAb or Tf in K^+-free isotonic buffer at 37^o for 1 h or 5 min, respectively. For cellular acidification experiments, the cells were incubated sequentially in serum-free DMEM supplemented with 25 mM NH_4Cl at 37^o for 30 min and in amiloride buffer containing 140 mM KCl/1 mM amiloride/40 mM Hepes acid pH 7.0 at 37^o for 2 min. The CD82 and Tf internalizations were then performed as described above in amiloride buffer. The endocytoses were quantified by assessing the percentage of transfected cells having either internalized CD82 or internalized Tf, respectively. The histograms represent the mean of four experiments ± SD. In each experiment, 60 cells were quantitated from each treatment. **B**. The steady-state distribution of CD82 was not altered by the dominant-negative Eps15. PC3-CD82 cells transfected with Eps15-DIII-GFP (the dominant-negative form of Eps15) or Eps15-DIIIΔ2-GFP (a control construct) were grown on coverslips overnight and then analyzed for CD82 distribution in immunofluorescence as described above. Digital images were captured with laser scan confocal microscopy at magnification of 63 X.

Figure S4 ARF6 is not required for CD82 internalization. **A**. Du145-CD82 and PrEC-NH cells transiently transfected with ARF6 wild type-GFP or ARF6 dominant negative mutant T27N-GFP were incubated with CD82 mAb M104 or TS82b or MHC class I mAb W6/32 at 4°C for 1 h and then switched to 37°C for 30 min for internalization. After acidic washes, the cells were further incubated with Alexa 594-conjugated goat anti-mouse IgG at RT for 1 h. Images of transverse Z-sections were captured by a confocal microscope. Scale bar, 10 μm. **B**. Quantitative analysis. Endocytosis was quantitated as either the percentage of the ARF6/GFP-expressing cells that contain the internalized MHC class I or CD82 from the total ARF6/GFP-expressing cells or the average numbers of MHC class I- or CD82-positive vesicles in each ARF6/GFP-expressing cell. In each experiment, approximately 20 Du145-CD82 or 100 PrEC-NH cells were quantitated from each group. The bars represent the mean of endocytoses from three to five experiments ± standard error. * denotes $P < 0.05$.

Figure S5 Effects of MβCD on the distributions of cholesterol and CD82 at the cell surface and the endocytosis of Tf. A. PrEC-NH and Du145-CD82 cells were treated with 5 mM MβCD at 37^oC for 60 min in serum-free media followed by 2 washes with PBS and fixation and then incubated with filipin (25 μg/ml) at RT for 30 min followed by 2 washes with

PBS. Fluorescent images were acquired under a deconvolution microscope. In MβCD-treated cells, filipin stains the cholesterol in intracellular vesicles because MβCD likely increased permeability of the plasma membrane to filipin. **B**. The cells were treated with MβCD as described above and then incubated with CD82 mAb, fixed, and further incubated with the 2nd Ab. Fluorescent images were acquired under a confocal microscope without confocality. **C.** PrEC-NH and Du145-CD82 cells were treated with or without MβCD (5 mM) at 37°C for 60 min. Tf endocytosis were analyzed as described in "Materials and Methods" by the incubation of Tf at 37°C for 5 min. Fluorescent images were acquired under a confocal microscope without confocality. Scale bar (in all images): 10 μm.

Figure S6 The distribution of CD82 proteins in the density fractions. Du145-CD82 cells were lysed in 1% Lubrol WX and fractionated in the discontinuous sucrose gradients as described in Materials and Methods. The fractions were collected, separated by nonreducing SDS-PAGE, and blotted in Western blot with CD82 mAb TS82b. The relative quantities of CD82 proteins in the fractions were determined by densitometry analysis and expressed as the bars, as indicated by the Y-axis on the left. The total protein in each fraction was assayed by the BCA method and presented in the curve, as indicated by the Y-axis on the right. The fractions 1 to 9 denote the fraction density from light to heavy.

Figure S7 Colocalization analysis of internalized CD82 and GPI-anchored proteins in Du145-CD82 cells. The Du145-CD82 cells that were transiently transfected with GFP-GPI construct were used for the colocalization between GFP-GPI and CD82 at 24 or 48 h after transfection. The colocalization of the internalized CD82 or Tf with GFP-GPI was quantitated as the percentage of the GFP-GPI-colocalized CD82- or Tf-positive vesicles per total CD82- or Tf-positive vesicles, respectively. Approximately 40 cells were quantitated for each treatment in each experiment. The results represent the mean of four experiments ± SEM.

Figure S8 The effect of latrunculin treatment on PrEC actin cytoskeleton. PrEC-NH cells were cultured on coverslips until 50% confluent. After being treated with DMSO or latrunculin A (1 μM) at 37°C for 1 h, the cells were fixed, permeabilized, and incubated with rhodamine-conjugated α-phalloidin at RT for 1 h. The digital images were obtained by confocal microscope. Scale bar, 10 μm.

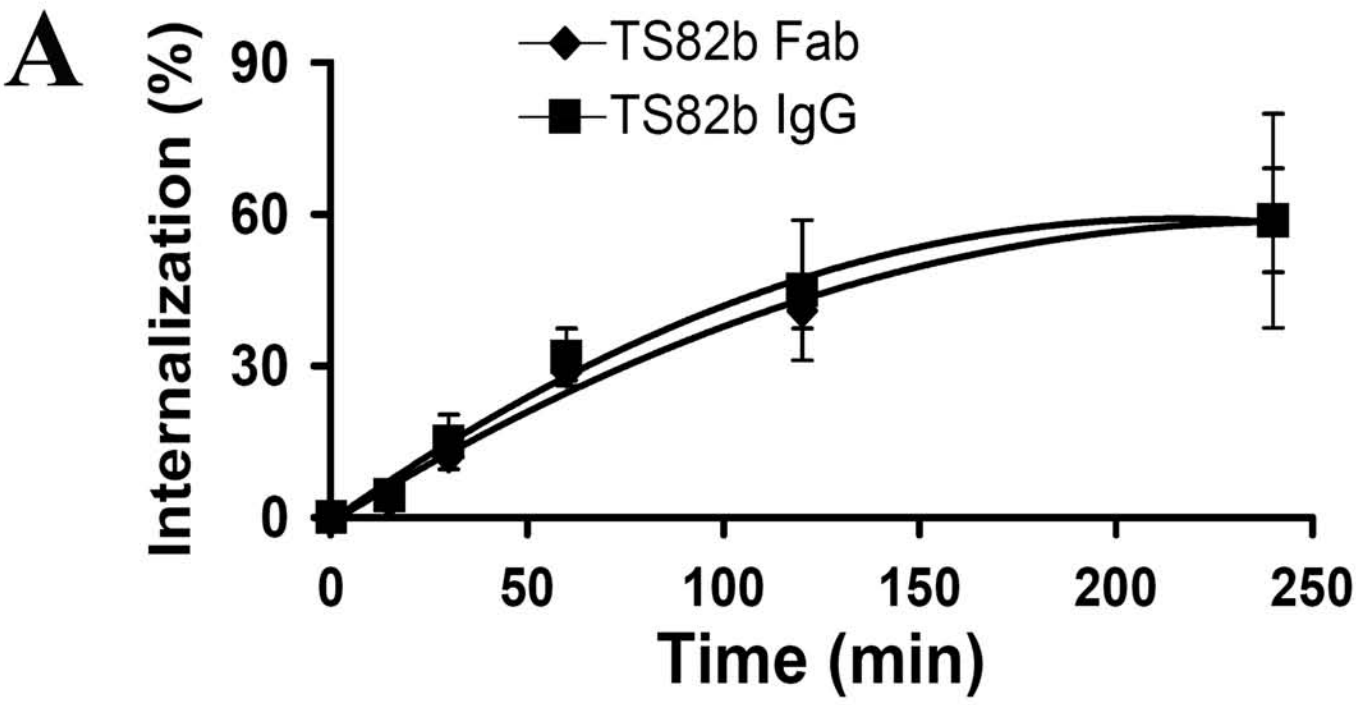
A
TS82b Fab
TS82b IgG
Internalization (%)
90
60
30
0
0
50
100
150
200
250
Time (min)

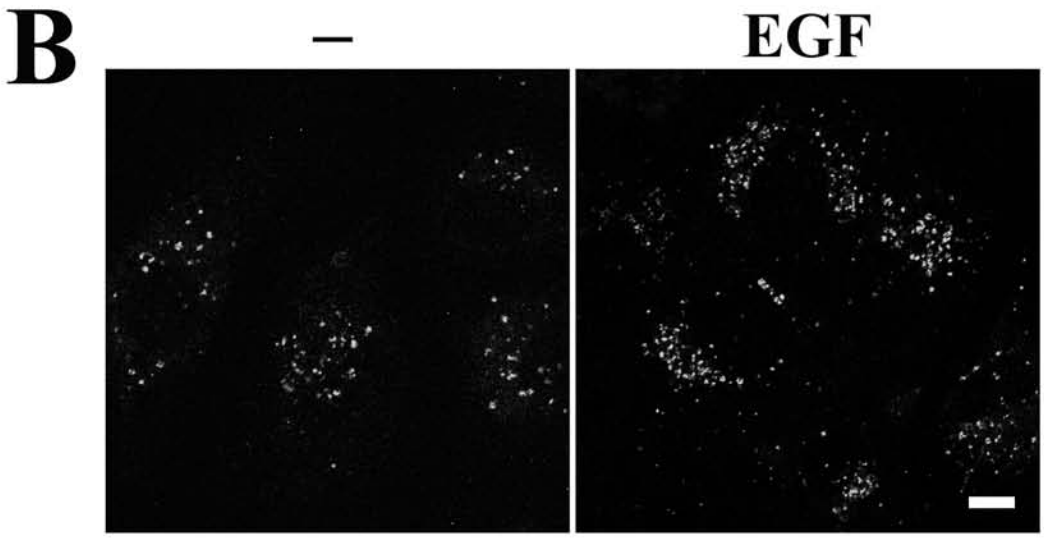
B
–
EGF

Figure S1

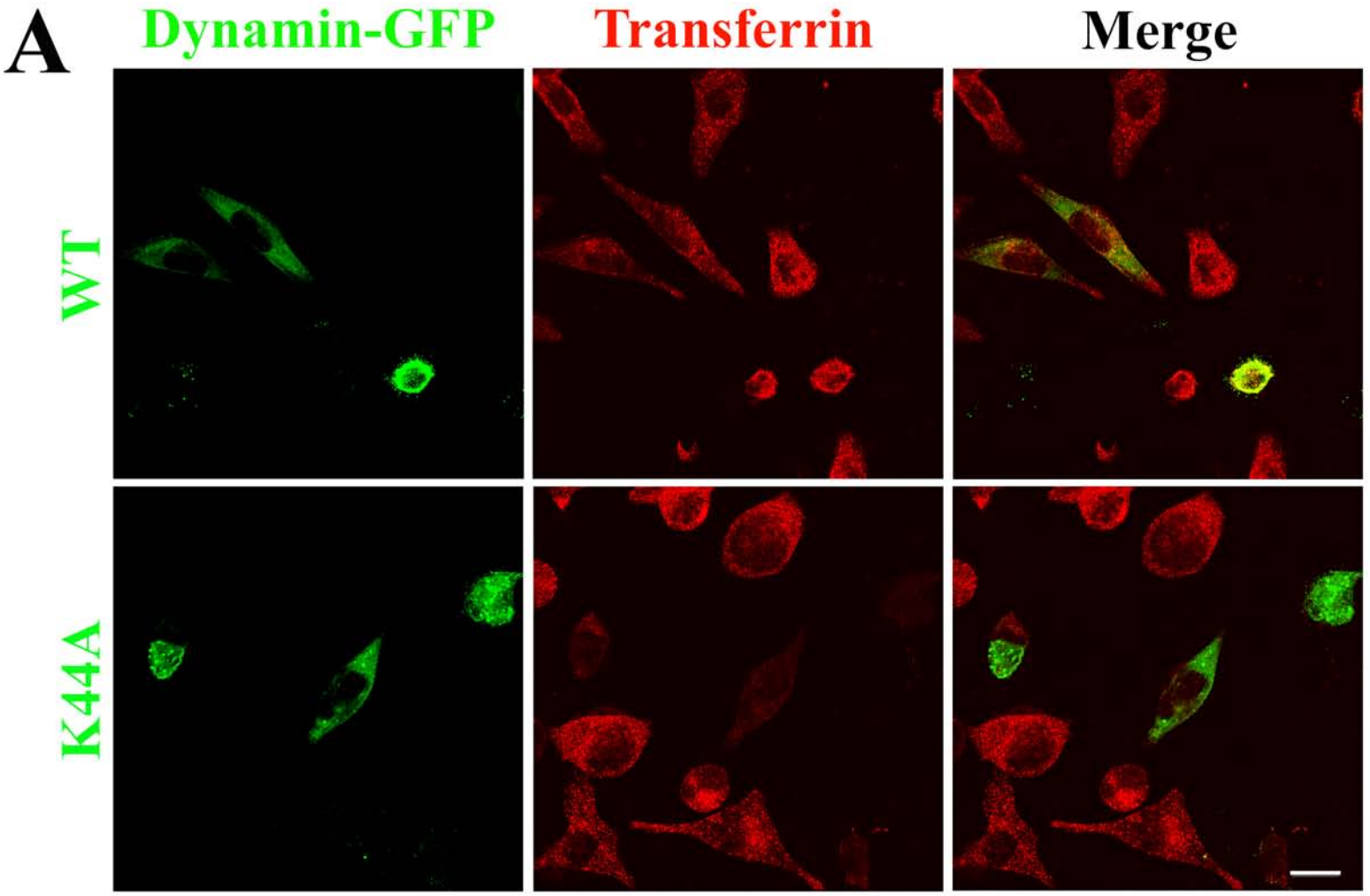
A
Dynamin-GFP
Transferrin
Merge
WT
K44A

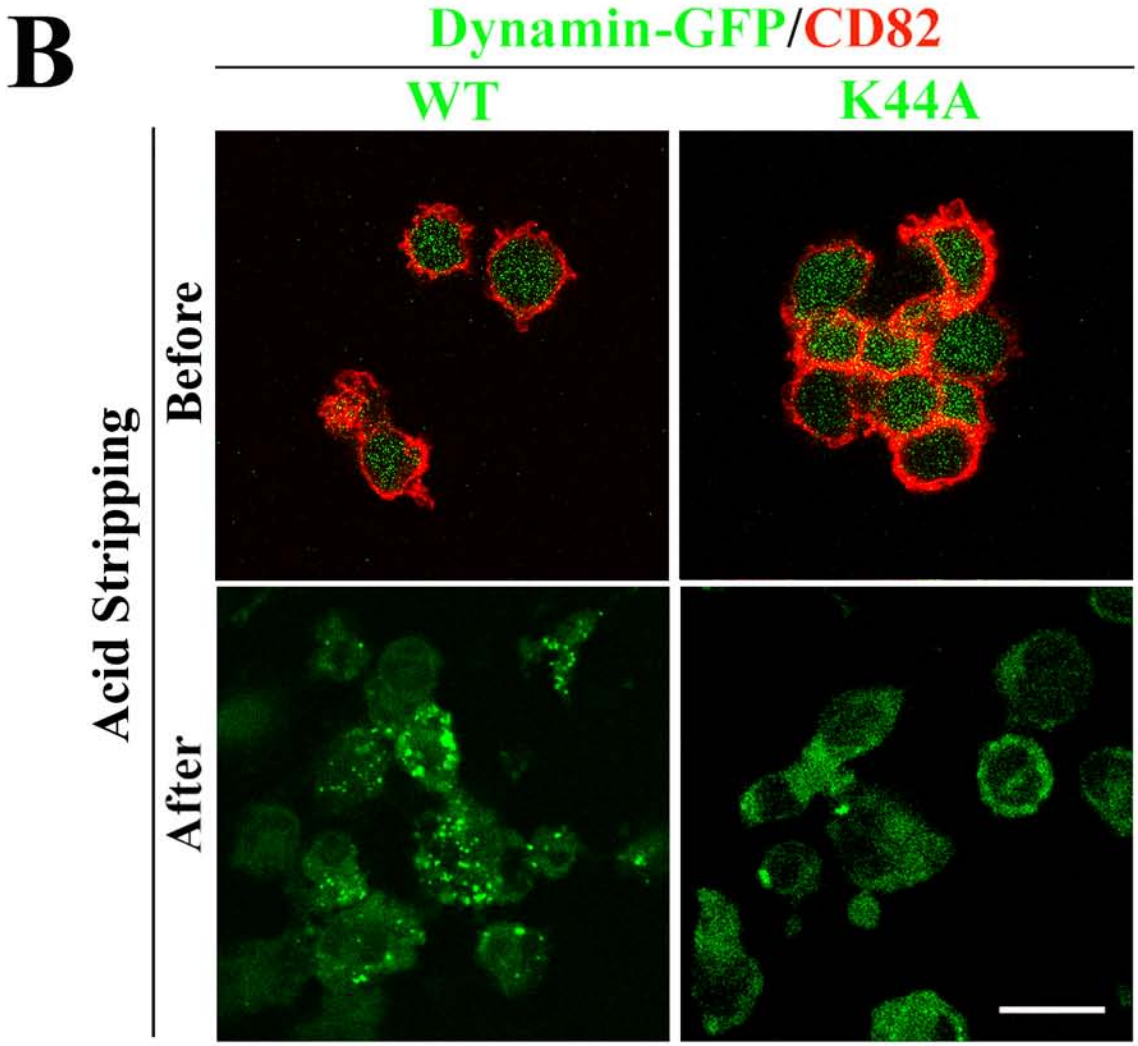
B
Dynamin-GFP/CD82
WT
K44A
Acid Stripping
Before
After

Figure S2

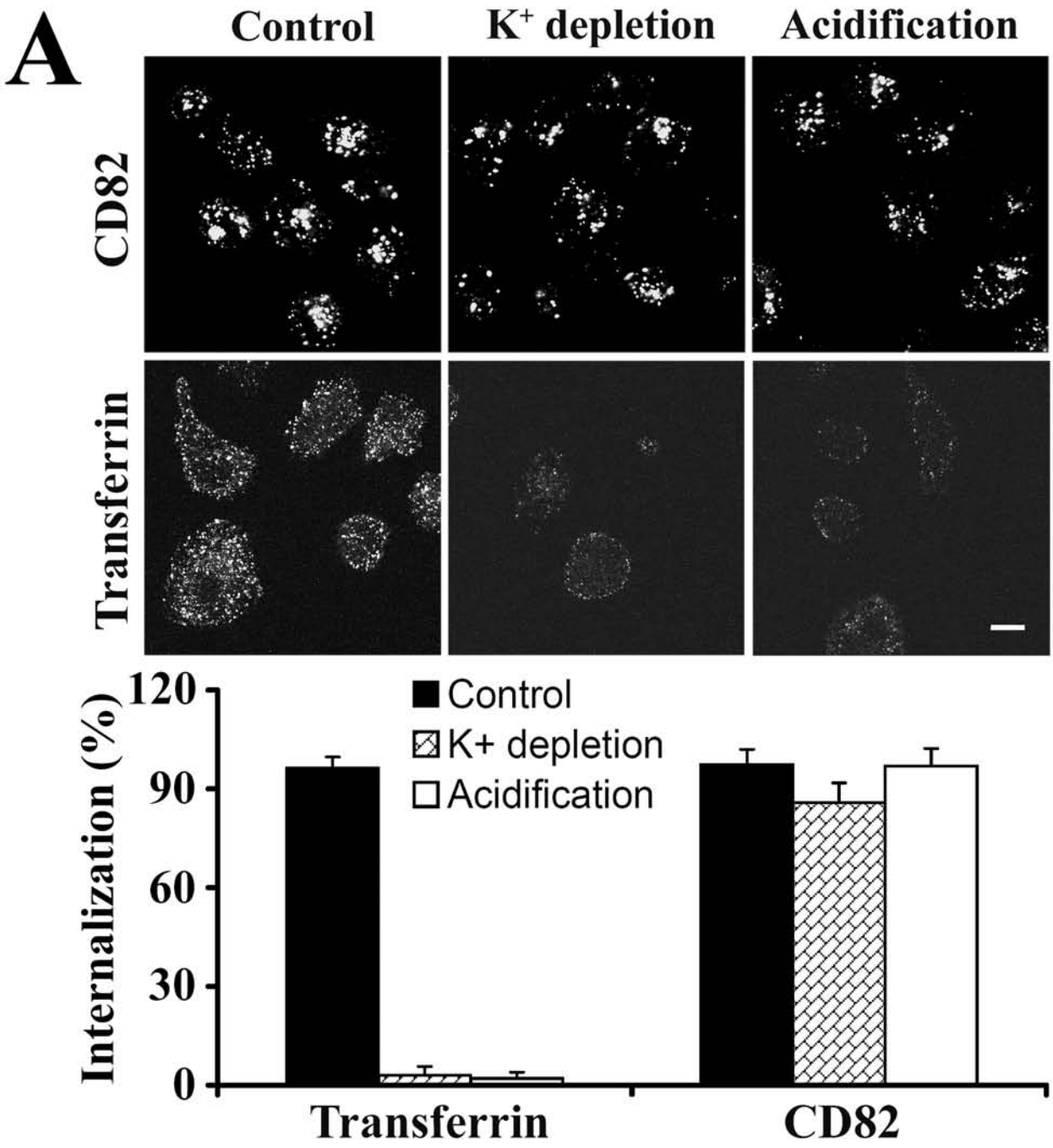
A
Control
K+ depletion
Acidification
CD82
Transferrin
Internalization (%)
120
90
60
30
0
Control
K+ depletion
Acidification
Transferrin
CD82

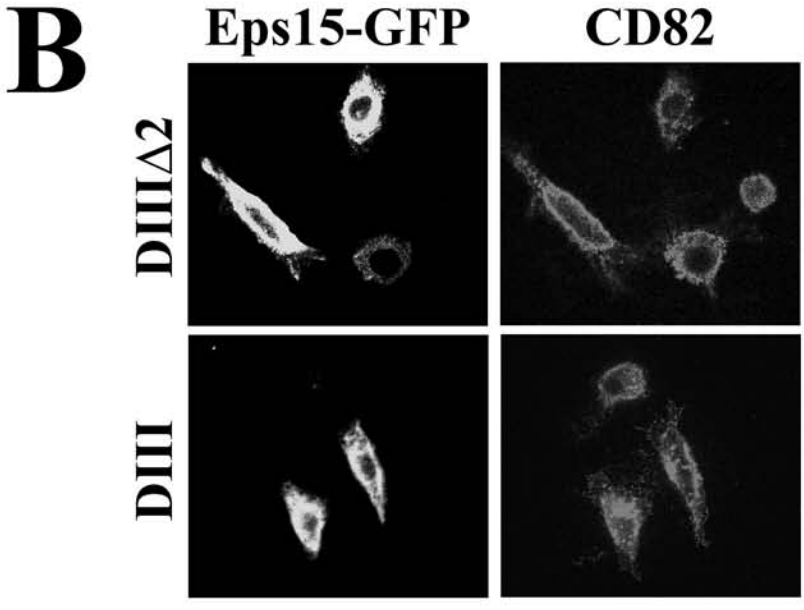
B
Eps15-GFP
CD82
DIIIΔ2
DIII

Figure S3

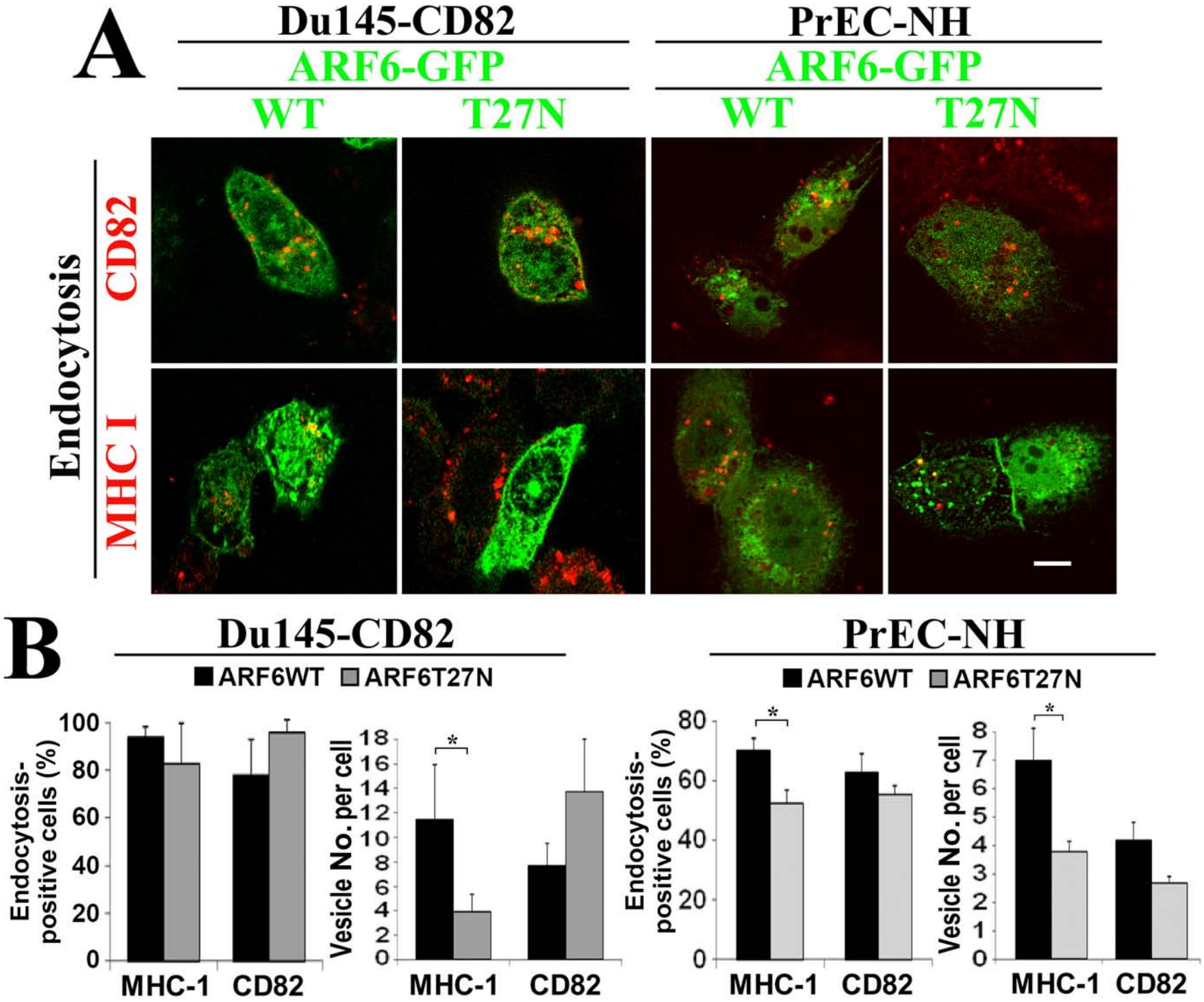
A
Du145-CD82
PrEC-NH
ARF6-GFP
ARF6-GFP
WT
T27N
WT
T27N
Endocytosis
CD82
MHC I
B
Du145-CD82
PrEC-NH
ARF6WT
ARF6T27N
ARF6WT
ARF6T27N
Endocytosis-positive cells (%)
Vesicle No. per cell
Endocytosis-positive cells (%)
Vesicle No. per cell
MHC-1
CD82
MHC-1
CD82
MHC-1
CD82
MHC-1
CD82

Figure S4

A
Control
MβCD
Filipin staining
PrEC-NH
Du145-CD82
B
Control
MβCD
CD82 staining
PrEC-NH
Du145-CD82
C
Control
MβCD
Transferrin Endocytosis
PrEC-NH
Du145-CD82

Figure S5

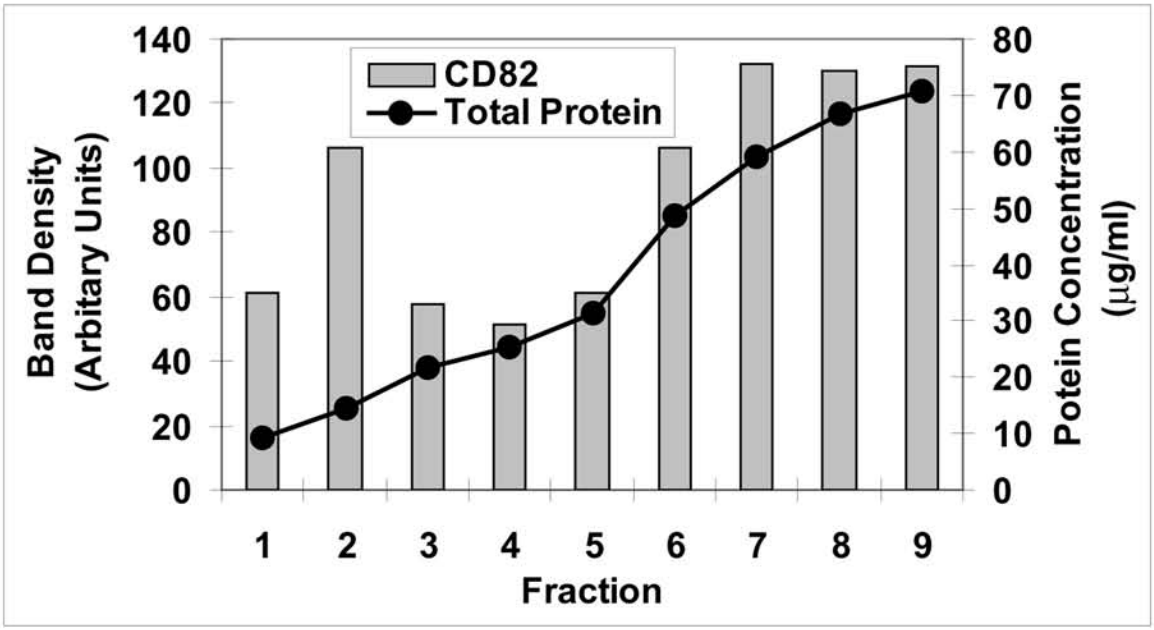
CD82
Total Protein
Band Density (Arbitary Units)
Potein Concentration (μg/ml)
Fraction
0
20
40
60
80
100
120
140
0
10
20
30
40
50
60
70
80
1
2
3
4
5
6
7
8
9

Figure S6

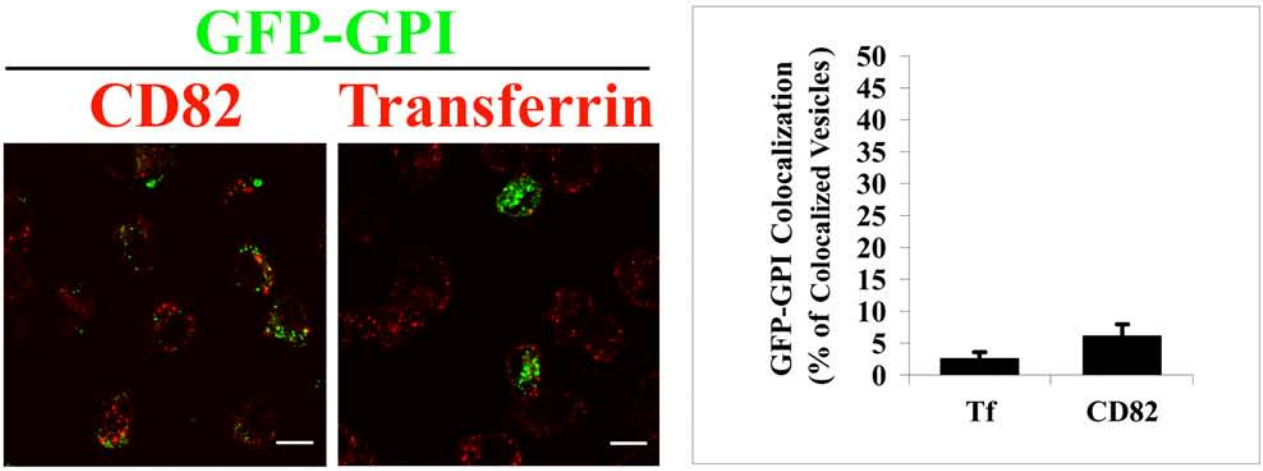
GFP-GPI
CD82
Transferrin
GFP-GPI Colocalization
(% of Colocalized Vesicles)
50
45
40
35
30
25
20
15
10
5
0
Tf
CD82

Figure S7

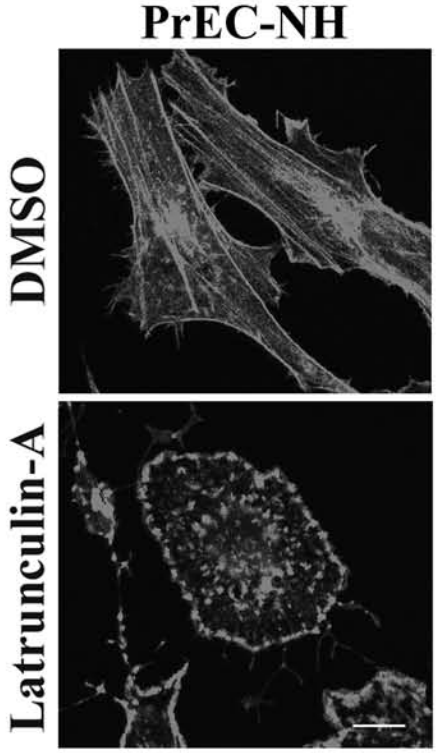

Figure S8